

# Holographic Krylov complexity for Yang-Baxter deformed supergravity backgrounds

---

**Dibakar Roychowdhury**<sup>a</sup>

<sup>a</sup>*Department of Physics, Indian Institute of Technology Roorkee,  
Roorkee 247667, Uttarakhand, India*

**ABSTRACT:** We compute the holographic Krylov complexity for a class of strongly coupled QFTs in a top down approach, where the dual gravitational counterpart corresponds to Yang-Baxter (YB) deformed supergravity solutions in a type IIB set up. The full 10d solution contains the  $AdS_n$  ( $n = 2, 3$ ) as the subspace, along with the dilaton and the background RR and NS fluxes. The Krylov complexity in the dual operator picture is obtained by computing the proper momentum of the massive particle along its geodesic in the bulk spacetime. We explore the effects of YB deformation on the bulk momentum of the particle, which in turn affects the rate of growth of complexity in the dual QFTs. Our results boil down into the undeformed case in the appropriate limit of the YB parameter.

---

## Contents

<b>1</b>	<b>Introduction and General Idea</b>	<b>1</b>
<b>2</b>	<b>Deformed <math>AdS_2 \times S^2 \times T^6</math> background in type IIB</b>	<b>4</b>
2.1	Embedding coordinates and the Krylov basis	4
2.2	Operator growth and Krylov complexity	5
2.2.1	The undeformed case	6
2.2.2	The YB effects	7
<b>3</b>	<b>Two parameter deformation of <math>AdS_3 \times S^3 \times T^4</math></b>	<b>9</b>
3.1	Supergravity solutions and Krylov basis	9
3.2	Operator growth and Krylov complexity	12
<b>4</b>	<b>Comments on the mirror model</b>	<b>14</b>
4.1	Krylov basis and geodesic motion	15
4.2	Proper momentum and Krylov complexity	16
<b>5</b>	<b>Summary and conclusions</b>	<b>17</b>

---

## 1 Introduction and General Idea

Chaotic systems are traditionally diagnosed by means of OTOC [1], which exhibits exponential growth characterized by the Lyapunov exponent. Another quantity that has recently drawn renewed attention in the context of quantum chaos is the Krylov complexity [2]-[5] and is the latest addition to existing models on complexity [6]-[8] in the literature. The Krylov complexity typically is the measure of how quickly an operator  $\mathcal{O}$  spreads over the Krylov subspace of the full Hilbert space under time evolution [9]-[12]. This might exhibit oscillatory, linear, or exponential growth for the chaotic system under consideration.

In this work, we shall be mostly aligned with the arguments of [13]-[21] which conjectures that the operator size growth in QFTs corresponds to the growth of radial momentum of the particle on the dual gravitational counterpart. We apply this idea to various deformed supergravity backgrounds and conjecture about the Krylov complexity associated with the dual-operator growth. According to conjecture [13]-[21], the rate of complexity growth is proportional to the momentum of the massive particle in the bulk spacetime

$$\partial_t \mathcal{C}(t) = -\frac{P_\rho}{\epsilon}. \quad (1.1)$$

The particle (of mass  $m$ ) is created near the boundary of the spacetime due to the insertion of an operator  $\mathcal{O}(t_0, x)$  at some particular instant of time ( $t_0$ ). As time progresses,

the size of the operator increases  $\mathcal{O}(t, x) = e^{iHt}\mathcal{O}(0, x)e^{-iHt}$ , resulting in a cascade of commutators and, therefore, in an increase in complexity ( $\mathcal{C}(t)$ ). In the dual gravity description, the particle starts to fall through the bulk without back-reacting on the geometry.

There have been two different approaches to the Krylov complexity in the context of holography. One of them is based on the above theme of computing the proper momentum of the particle along the geodesic [22]-[30], while the other is based on the notion of the rate of growth of the wormhole length in the dual gravity description [31]-[35]. The reader is also encouraged to refer to [36]-[38] for a nice set of comprehensive reviews on the subject.

As emphasized above, in this paper, we focus solely on the Krylov complexity [2] growth associated with the operator spectrum in dual QFTs following the former line of approach. In particular, we extend the arguments of [24] to compute the Krylov complexity growth for a class of Yang-Baxter (YB) deformed supergravity backgrounds [39]-[51].

We begin by discussing the Yang-Baxter (YB) deformed  $AdS_2 \times S^2 \times T^6$  in 10d [39]-[40]. These are the solutions in type IIB supergravity constructed using unimodular R-matrices. We show that these YB deformed geometries are *conformally* equivalent to the conventional Krylov basis [24] where the conformal/scale factor explicitly depends on the YB deformation parameter. To simplify calculations, we consider a particular geodesic where the background dilaton becomes a trivial factor; as a result the string and the Einstein frame are the same.

In the subsequent analysis, we generalize the above result by uplifting the QFT in one higher dimension whose dual gravitational counterpart corresponds to a supergravity solution with a pure  $AdS_3$  factor plus deformations due to YB effects. These backgrounds are generated through unimodular  $R$ -matrices that depend on the deformation parameters ( $\kappa_{\pm}$ ) associated with each copy of the superisometry algebra of the undeformed  $AdS_3 \times S^3 \times T^4$  [41]-[42]. Depending on the choice of the  $R$ -matrix (with all fermionic roots), two different supergravity solutions are obtained. One of these deformed backgrounds allows for a mirror dual, which we also explore towards the end of this paper. As these backgrounds are manifested as deformations of the standard  $AdS_3$  background, they bring up some non-trivial modification to the standard  $SL(2, R)$  Krylov spin chain [24]. These modifications on the field theory side are in one to one correspondence with the YB deformation in the bulk, and their effects can be seen in a non-trivial fashion within the holographic setup.

The purpose of our analysis is in particular to explore the effects of YB deformation on the Krylov complexity growth of operators in dual QFTs. To see this explicitly, we compute the proper momentum ( $P_{\rho}$ ) of the particle as a function of time ( $t$ ) and calculate its variation for different choices of the YB parameter. In our first example of deformed  $AdS_2 \times S^2 \times T^6$ , we see that the effects due to YB deformations can be interpreted from the perspective of the undeformed theory as a particle moving with a finite initial velocity near the boundary, which corresponds to a non-zero rate of growth of complexity to begin with (see Fig.1). The effect of YB deformation is to introduce a finite radial cut-off in the bulk, which reduces the effective dimensionality of the Krylov basis in the dual CFT. Almost identical features are observed for the two parameter deformation of the  $AdS_3 \times S^3 \times T^4$  background [42], except for the non-trivial fact that in this particular example, one can perform analytic calculations with a very careful choice of deformation parameters ( $\kappa_L$  and  $\kappa_R$ ) setting both of them non-zero and very close to each other. It turns out that in this

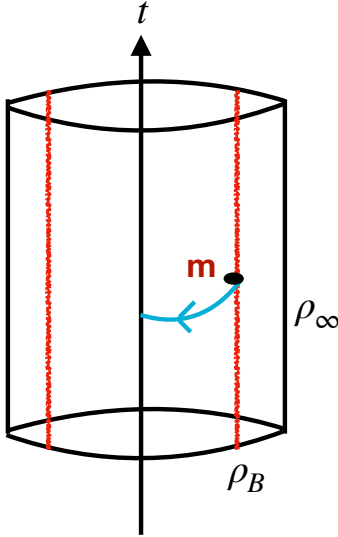


**Figure 1.** In the Figure above we picturize the geodesic motion of a massive particle (of mass  $m$ ) in the Yang-Baxter (YB) deformed background in global coordinates. The “holographic screen” (which could be thought of as an *effective* boundary of the spacetime) is located at finite radial distance  $\rho_B$ , which acts like a radial cut-off in the bulk AdS. Here,  $\rho_\infty$  is the location of the true asymptotic boundary of the (undeformed) AdS. From the perspective of an observer sitting at  $\rho_\infty$ , the massive particle is created at  $\rho_A \sim \rho_B$ , which is therefore always at a finite radial distance from the true boundary of the AdS spacetime and is identified with a finite momentum to begin with. The YB deformation reduces the *proper* geodesic distance of the massive particle trajectory in the bulk and hence the rate of complexity growth for the dual QFT living on  $\rho_\infty$ .

particular limit  $\kappa_L \sim \kappa_R$ , the geodesic of the massive particle in the dual geometry probes an  $SL(2, R)$  sector, which is therefore identified as the Krylov basis [24] in the dual QFT.

The mirror model is indeed quite different from its parent theory. To identify the Krylov basis, one has to perform a double Wick rotation and thereby an expansion in coordinates. It appears that the background has an exact  $SL(2, R)$  symmetry for zero deformation and corresponds to a 2d CFT on a thermal cycle with periodicity  $\beta = 2\pi$ . However, in the presence of finite YB effects, one deviates from this ideal situation. In all three cases, we find a suppression of the rate of complexity growth with increasing YB deformation.

The organization of the rest of the paper is as follows. In Section 2, we identify the dual Krylov basis and the associated complexity for YB deformed  $AdS_2 \times S^2 \times T^6$  solution in type IIB supergravity. We extend them for two parameter deformed  $AdS_3 \times S^3 \times T^4$  solution in Section 3, where identify the appropriate Krylov basis in a particular limit of the deformation parameters. We consider the mirror model in Section 4 and show that the dual Krylov basis can be obtained following a double Wick rotation. Finally, we summarize our results in Section 5 and conclude this paper with some future remarks.

## 2 Deformed $AdS_2 \times S^2 \times T^6$ background in type IIB

In the first part, we review the essential details about the background and its deformations. Next, we find perturbative solutions for the momentum ( $P_\rho$ ) of the bulk particle, which is dual to an operator insertion in the UV field theory at the initial time  $t \sim 0$ . We plot the proper momentum ( $P_\rho$ ) as a function of time that exhibits linear growth at early times.

### 2.1 Embedding coordinates and the Krylov basis

We begin by reviewing the deformed  $AdS_2 \times S^2 \times T^6$  background in type IIB supergravity. These classes of geometries are constructed based on the notion of YB deformation [54]-[55] of the  $AdS$  coset sigma model and is a generalization of the YB deformation of the Principal Chiral Model (PCM) [56]-[57]. The deformation is introduced by means of an  $R$ -matrix that satisfies the non-split modified YB- equation on the superisometry algebra  $\mathfrak{psu}(1, 1|2)$  of the undeformed background. It turns out that the resulting geometry, the dilaton, and the background fluxes solve a type IIB equation when all the simple roots of the Dynkin diagram are fermionic [39]. This in turn is related to the *unimodularity* of the  $R$ -matrix as suggested in [58]. The resulting  $R$ -matrices (known as Drinfel'd-Jimbo  $R$ -matrices) correspond to a  $q$ -deformation of the super-isometry algebra [59]-[60].

The corresponding metric (in the string frame) can be expressed as [39]

$$ds_{10}^2 = ds_4^2 + ds_{T^6}^2 \quad (2.1)$$

$$ds_4^2 = \frac{L^2}{(1 - \kappa^2 \varrho^2)} \left( -(1 + \varrho^2) dt^2 + \frac{d\varrho^2}{(1 + \varrho^2)} \right) + \frac{L^2}{(1 + \kappa^2 r^2)} \left( (1 - r^2) d\phi^2 + \frac{dr^2}{(1 - r^2)} \right) \quad (2.2)$$

$$ds_{T^6}^2 = L^2 d\varphi_i d\varphi_i ; \quad \kappa = \frac{2\eta}{1 - \eta^2} ; \quad i = 4, \dots, 9 \quad (2.3)$$

where  $\kappa \in [0, \infty]$  is the YB deformation parameter.

The dilaton associated with the background (2.1)-(2.3) is given by

$$e^{-2\Phi} = e^{-2\Phi_0} \frac{(1 - \kappa^2 \varrho^2)(1 + \kappa^2 r^2)}{1 - \kappa^2(\varrho^2 - r^2 - \varrho^2 r^2)}. \quad (2.4)$$

To proceed further, we switch off the coordinates  $\varphi_i \in T^6$  as they are not relevant for our analysis. Moreover, we restrict the geodesic of the massive particle in (deformed)  $AdS_2$  where we set the angles on the two sphere as constants, namely  $r = 0$  and  $\phi = \text{constant}$ . This trivially fixes the dilaton  $e^{-2\Phi} = e^{-2\Phi_0} = \text{constant}$ . In other words, the metric in the string frame is effectively the same as in the Einstein frame  $ds_E^2 = e^{-\frac{\Phi_0}{2}} ds_{\text{string}}^2$ .

This finally yields the 2d metric in the Einstein frame as (after a rescaling by  $e^{\frac{\Phi_0}{2}}$ )

$$ds_E^2 = \frac{L^2}{(1 - \kappa^2 \varrho^2)} \left( -(1 + \varrho^2) dt^2 + \frac{d\varrho^2}{(1 + \varrho^2)} \right) \quad (2.5)$$

which serves as the starting point for our subsequent analysis.

Notice that the background (2.5) is conformally equivalent to pure  $AdS_2$  and smoothly transits into it in the limit  $\kappa \rightarrow 0$ . We now move on to the Krylov basis ( $|K_n\rangle$ ) in a few steps. As a first step, we introduce  $\tilde{\varrho} = \arctan \varrho$  and rewrite (2.5) as (we set  $L = 1$ )

$$d\tilde{s}_E^2 = \Omega(\tilde{\varrho})(-dt^2 + d\tilde{\varrho}^2) ; \Omega(\tilde{\varrho}) = \frac{1}{\cos^2 \tilde{\varrho} - \kappa^2 \sin^2 \tilde{\varrho}}. \quad (2.6)$$

In order to express the 2d metric (2.6) in an appropriate radial coordinate ( $\rho$ ), which is conjectured to be the dual of the Krylov basis  $|K_n\rangle$  associated with the 1d chain [24], we introduce the following change of variables:

$$\cos \tilde{\varrho} = \frac{1}{\cosh \rho} \quad (2.7)$$

which finally yields the 2d metric in the desired form

$$d\tilde{s}_E^2 = \Omega(\rho)(-\cosh^2 \rho dt^2 + d\rho^2) ; \Omega(\rho) = \frac{1}{1 - \kappa^2 \sinh^2 \rho}. \quad (2.8)$$

The background (2.8) is conformally equivalent to a  $(0 + 1)$ d CFT on a finite length  $l = 2\pi$ . Notice that the conformal factor  $\Omega(\rho)$  diverges at

$$\rho_B = \sinh^{-1} \left( \frac{1}{\kappa} \right) ; \kappa > 0 \quad (2.9)$$

which defines the location of the holographic screen (or the *effective* boundary of the spacetime) [61]-[62]. A closer inspection reveals that the location of the effective boundary (2.9) shifts more towards the true boundary as  $\kappa \sim 0$ , which is the undeformed spacetime.

## 2.2 Operator growth and Krylov complexity

We perform analysis for the most generic value of the deformation parameter ( $\kappa$ ). The particle is created near the screen ( $\rho \sim \rho_B$ ) and as it probes deep inside the bulk, it corresponds to Krylov complexity growth at later times. The idea would be to compute the proper radial momentum ( $P_\rho$ ) (which corresponds to the complexity growth (1.1)) and plot it as a function of time ( $t$ ) for different choices of the YB deformation parameter ( $\kappa$ ).

The geodesic of the massive particle follows from the action

$$S = -m \int dt \sqrt{-g_{\mu\nu} \dot{x}^\mu \dot{x}^\nu}. \quad (2.10)$$

Using (2.8), one finds the following action for the massive particle

$$S = \int dt L ; L = -m \sqrt{\Omega(\rho)(\cosh^2 \rho - \dot{\rho}^2)}. \quad (2.11)$$

The radial momentum of the particle can be expressed as

$$P_\rho = \frac{m \dot{\rho} \sqrt{\Omega(\rho)}}{\sqrt{\cosh^2 \rho - \dot{\rho}^2}}. \quad (2.12)$$

The Hamiltonian constraint, on the other hand, yields

$$H = H_0 = P_\rho \dot{\rho} - L = \frac{m \cosh^2 \rho \sqrt{\Omega(\rho)}}{\sqrt{\cosh^2 \rho - \dot{\rho}^2}}. \quad (2.13)$$

Using (2.13), we can further simplify (2.12) as

$$P_\rho = \frac{H_0 \dot{\rho}}{\cosh^2 \rho}. \quad (2.14)$$

Finally, we note down the equation of motion for  $\rho(t)$ , which turns out to be

$$\frac{d}{dt} \left( \frac{\sqrt{\Omega} \dot{\rho}}{\sqrt{\cosh^2 \rho - \dot{\rho}^2}} \right) + \frac{\sqrt{\Omega} \sinh 2\rho}{2\sqrt{\cosh^2 \rho - \dot{\rho}^2}} + \frac{\partial_t \Omega}{2\dot{\rho} \sqrt{\Omega}} \sqrt{\cosh^2 \rho - \dot{\rho}^2} = 0. \quad (2.15)$$

A closer look reveals that (2.15) is equivalent to setting the time derivative of the constraint (2.13) equal to zero, that is,  $\frac{dH_0}{dt} = 0$ . We therefore choose to work with the constraint condition (2.13), which after some simplification yields (with  $m = 1$ )

$$\dot{\rho}^2 = \cosh^2 \rho \left( 1 - \frac{\cosh^2 \rho}{H_0^2} \Omega(\rho) \right). \quad (2.16)$$

### 2.2.1 The undeformed case

Let us first revisit the undeformed case [24] which sets  $\Omega = 1$ . Taking into account that the particle starts with zero velocity *near* the boundary  $\rho = \rho_\infty$  at initial time ( $t = 0$ ), we fix the constant of motion ( $H_0$ ) in terms of the location of the asymptotic boundary ( $\rho = \rho_\infty$ )

$$H_0^2 = \cosh^2 \rho_\infty \quad (2.17)$$

which is a large number in the true asymptotic limit  $\rho_\infty \rightarrow \infty$ .

This yields the following differential equation

$$\dot{\rho}^2 = \frac{\cosh^2 \rho}{\cosh^2 \rho_\infty} (\cosh^2 \rho_\infty - \cosh^2 \rho). \quad (2.18)$$

Taking into account that  $\rho_\infty \rightarrow \infty$ , the above eq. (2.18) yields the following solution

$$\tan^{-1}(\sinh \rho) = \frac{\pi}{2} - t + \mathcal{O}(H_0^{-2}) \quad (2.19)$$

where the integration constant ( $= \frac{\pi}{2}$ ) can be determined by setting  $\rho = \infty$  at  $t = 0$ . Notice that when  $t = t_f = \frac{\pi}{2}$ , the particle reaches the center ( $\rho = 0$ ) of  $AdS_2$ .

One could rewrite the solution (2.19) in the form of [24]

$$\cos^{-1}(\tanh \rho) = t \Rightarrow \rho(t) = \rho_\infty \tanh^{-1}(\cos t) + \mathcal{O}(H_0^{-2}) \quad (2.20)$$

where the dual Krylov chain has a finite length  $l = 2\pi$  (also see eq. (2.8)).

It turns out that, for the purpose of our subsequent discussion on YB effects, it would be important to estimate the above entity in eq. (2.18) up to NLO

$$\tan^{-1}(\sinh \rho) + \frac{1}{2H_0^2} \sinh \rho = \frac{\pi}{2} - t - \frac{C}{H_0^2} \equiv \hat{t}_f - t. \quad (2.21)$$

Clearly, with sub-leading corrections in action, the boundary is not strictly located at  $\infty$  and therefore the particle takes a shorter time ( $\hat{t}_f < t_f$ ) to reach the center of  $AdS_2$ . After some simple algebra, it is straightforward to obtain the solution

$$\sinh \rho = \alpha \cot \left( t + \frac{C}{H_0^2} \right); \quad \alpha = 1 - \frac{1}{2H_0^2} \quad (2.22)$$

which is the generalization of (2.19) in the presence of a finite radial cut-off.

### 2.2.2 The YB effects

In the context of pure  $AdS_2$ , the above analysis does not make much sense since the constant of motion  $H_0 = \infty$  and the boundary is strictly located at asymptotic infinity. However, in the presence of the YB deformation, the boundary (or the holographic screen) is located at a finite radial cut-off (2.9) depending on the value of the deformation parameter ( $\kappa$ ).

Like before, by considering the fact that the particle is created near the holographic screen at  $\rho \sim \rho_\Lambda \sim \rho_\infty$ , we find the velocity of the particle for small deformation ( $\kappa \ll 1$ )

$$\dot{\rho} = \kappa \cosh \rho \sinh \rho|_{\rho \sim \rho_\Lambda} + \mathcal{O}(\kappa^2) \quad (2.23)$$

where  $\rho_\Lambda < \rho_B$ . In other words, the effect of YB deformation ( $\kappa \neq 0$ ), is to set a non-zero (small but *finite*) value for the radial velocity ( $\dot{\rho} < 1$ ) and hence the proper momentum ( $P_\rho$ ), which brings a crucial difference with the analysis in the undeformed case.

In order to explore the effects of the YB deformation on the Krylov complexity, one has to take into account the terms at  $\mathcal{O}(H_0^{-2})$ , which yields an integral equation of the form

$$\int \frac{d\rho}{\cosh \rho} + \frac{1}{2\kappa H_0^2} \int d\rho \frac{\cosh \rho}{1 - \kappa^2 \sinh^2 \rho} + S_{ct} = \hat{t}_f - t \quad (2.24)$$

where  $\hat{t}_f$  is the time that the particle takes to reach the center of  $AdS_2$ .

Notice that the second integral diverges near the boundary  $\rho = \rho_B$ . On the other hand, in the limit  $\kappa \rightarrow 0$ , one precisely recovers the undeformed eq. (2.19). The YB effect therefore amounts to a regularization and the addition of a counter term. After performing a careful analysis of the integral, one finds the counter term of the following form

$$S_{ct} = -\frac{a}{2\kappa H_0^2} \lim_{\rho \rightarrow \rho_B} \int_{\rho \sim \rho_B} d\rho \frac{\cosh \rho}{1 - \kappa^2 \sinh^2 \rho} = \frac{a}{4\kappa^2 H_0^2} \int_{z \sim \epsilon} \frac{dz}{z} = \frac{a}{4\kappa^2 H_0^2} \log \epsilon \quad (2.25)$$

where  $a$  is the appropriate pre-factor that we fix below in order to cancel the divergence. Here, in the above derivation, we use the fact that near the holographic screen  $1 - \kappa^2 \sinh^2 \rho|_{\rho \sim \rho_B} = 2(1 - \kappa \sinh \rho)|_{\rho \sim \rho_B}$ , where  $\rho_B$  is defined in (2.9).

Using (2.25) and performing the integral in eq. (2.24), we obtain the following relation

$$\tan^{-1}(\sinh \rho) + \frac{1}{2\kappa H_0^2} \tanh^{-1}(\kappa \sinh \rho) + S_{ct} = \hat{t}_f - t. \quad (2.26)$$

After a careful analysis, it can be shown that the time for the massive particle to reach the center of  $AdS_2$  turns out to be<sup>1</sup>

$$\hat{t}_f = \tan^{-1}(1/\kappa) + \frac{1}{2\kappa H_0^2} \tanh^{-1}(1 - z)|_{z \sim \epsilon} + S_{ct} = \tan^{-1}(1/\kappa) + \frac{\log 2}{4\kappa H_0^2} \quad (2.27)$$

<sup>1</sup>In what follows, in the subsequent analysis, we always absorb the counter term (2.25) in the definition of  $\hat{t}_f$ , meaning that the resulting entity is always finite.

where the second term is purely sourced due to YB correction in bulk supergravity. Notice that in order to cancel the divergence in eq. (2.27), one has to set  $a = \kappa$ . Finally, it should be noted that in the limit  $\kappa \rightarrow 0$ , one recovers the undeformed theory (2.19). This can be seen by taking the limit  $\kappa \rightarrow 0$  in the second term in (2.27), where we denote the Hamiltonian constraint near the boundary as  $H_0^2 = \cosh^2 \rho \Omega(\rho) \Big|_{\rho \sim \rho_B} = (1 + \kappa^{-2}) \Omega(\rho) \Big|_{\rho \sim \rho_B}$ .

**Small deformation limit.** An exact analytical solution of eq. (2.26) is a nontrivial task. However, a solution can be obtained in the limit where the YB effects are small enough to consider a perturbative expansion in the parameter  $\kappa (\ll 1)$ . This yields the following

$$\tan^{-1}(\sinh \rho) + \frac{\kappa^2}{2} \sinh \rho = \hat{t}_f - t \quad (2.28)$$

where the time to reach the bulk interior turns out to be

$$\hat{t}_f = \frac{\pi}{2} - |\kappa| + \frac{\kappa}{4} \log 2 + \mathcal{O}(\kappa^3) = \frac{\pi}{2} - \beta ; \beta = |\kappa| - \frac{\kappa}{4} \log 2 + \mathcal{O}(\kappa^3) \quad (2.29)$$

Notice that the time (2.29) to reach the center of the bulk is shorter compared to the undeformed case (2.19). This comes from the fact that the boundary is now shifted towards the interior and is at a finite radial cut-off depending on the value of the YB parameter ( $\kappa$ ).

Finally, we have a solution for the radial coordinate

$$\rho(t) = \tanh^{-1} \left( \frac{\gamma \cot \bar{t}}{\sqrt{1 + \gamma^2 \cot^2 \bar{t}}} \right) \quad (2.30)$$

$$\bar{t} = t + \beta ; \gamma = (1 + \frac{\kappa^2}{2})^{-1} \quad (2.31)$$

that smoothly transits into the undeformed solution (2.20), in the limit  $\kappa \rightarrow 0$ .

Using (2.30), we finally express the proper momentum (2.14) as<sup>2</sup>

$$P_\rho / H_0 = - \frac{\gamma \csc^2(\beta + t)}{(\gamma^2 \cot^2(\beta + t) + 1)^{3/2}}. \quad (2.32)$$

Setting  $\gamma = 1$  and  $\beta = 0$  in (2.32), one recovers the results of [24]

$$P_\rho / H_0 = - \sin t \quad (2.33)$$

in units where  $m = 1$  and  $l = 2\pi$ , which we have set at the beginning of our computation.

A closer observation reveals that the effect of the YB deformation is to reduce the rate of growth of Krylov complexity, which is also shown in Fig.2. This can be understood as a fact that the span of the radial direction ( $\rho$ ) becomes smaller with a larger deformation, which reduces the effective dimension of the Hilbert space associated with the Krylov basis.

Finally, as a second important observation and as also discussed below eq.(2.23), we notice that the particle must have a non-zero proper momentum (near the location of the

---

<sup>2</sup>Here,  $H_0$  keeps the information about the UV scale of the dual theory [24].

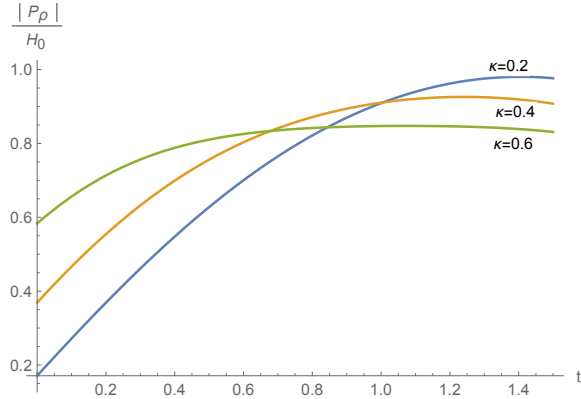


**Figure 2.** We show the rate of growth of Krylov complexity for various choices of the YB deformation parameter ( $\kappa$ ).

holographic screen) in order to see the effects due to YB deformation, which is shown in Fig.2 and can be seen from the following expansion of (2.30)

$$\begin{aligned}
 -P_\rho/H_0 &= \sin t - \frac{\kappa}{4} \cos t (-4 + \log 2) \\
 &+ \frac{\kappa^2}{32} \sin t (24 \cos(2t) - 8 - \log^2 2 + \log(256)) + \mathcal{O}(\kappa^3)
 \end{aligned} \tag{2.34}$$

which is non-zero at the initial time  $t = 0$  and is proportional to  $\kappa$ .

One way to interpret the above result is to argue that the YB deformation captures a subspace of the full Hilbert space associated with Krylov complexity growth. The time at which one starts measuring the complexity growth is not the true initial time. From the perspective of the *undeformed* theory on the dual gravity side, this can be understood by noting the fact that the YB deformation forces the particle to be *detected* at a finite radial distance from the true asymptotic boundary at infinity. As a result, the particle is found with a finite momentum that corresponds to a non-zero complexity growth to begin with.

### 3 Two parameter deformation of $AdS_3 \times S^3 \times T^4$

These backgrounds are in spirit similar to those discussed in the previous section, in the sense that they are obtained as a result of integrable deformation of type II Green-Schwarz (GS) superstrings by means of  $R$ -matrices satisfying non-split modified classical YB equation on the super-isometry algebra of the undeformed background. Like in the previous example, these  $R$ -matrices satisfy the unimodularity condition that ensures a supergravity solution as a target space geometry of the string. Below, we review different supergravity solutions [42] and thereby proceed towards constructing a possible Krylov basis for it.

#### 3.1 Supergravity solutions and Krylov basis

To begin with,  $AdS_3 \times S^3 \times T^4$  superstrings allow a superisometry algebra to be in the form of a product  $\hat{G}_L \times \hat{G}_R$ , which allows for a two parameter deformation [41], much similar in

spirit as that of the bi-Yang-Baxter deformation of the sigma model [63]. Corresponding to each copy of the superisometry algebra, one can introduce a real deformation parameter  $\kappa_L$  or  $\kappa_R$ , which results in a two parameter family of integrable deformations of type II GS superstrings and an associated supergravity solution. Each family of supergravity solution corresponds to a particular unimodular  $R$ -matrix associated with fully fermionic Dynkin diagram. Interestingly, one of these backgrounds exhibits *mirror* symmetry [53]. We explore the complexity growth for the mirror background towards the end of this paper.

The superisometry algebra we are interested in is constructed using one copy of the supergroup  $\hat{G} = PSU(1, 1|2)$ , which corresponds to strings moving in  $AdS_3 \times S^3 \times T^4$  in the presence of background fluxes. There happen to be two inequivalent classes of unimodular  $R$ -matrices, giving rise to two distinct classes of supergravity solutions that have a unique metric and different dilaton profiles [42]. For our purpose, we ignore the background RR and the NS fluxes. These backgrounds can be classified as follows:

**Class I background.** The metric and the dilaton are given by

$$ds_{10}^2 = \frac{1}{F(\varrho)} \left[ -(1 + \varrho^2)(1 + \kappa_-^2(1 + \varrho^2))dt^2 + \frac{d\varrho^2}{(1 + \varrho^2)} + \varrho^2(1 - \kappa_+^2\varrho^2)d\psi^2 \right. \\ \left. + 2\kappa_-\kappa_+\varrho^2(1 + \varrho^2)dtd\psi \right] + \frac{1}{\tilde{F}(r)} \left[ (1 - r^2)(1 + \kappa_-^2(1 - r^2))d\varphi^2 + \frac{dr^2}{1 - r^2} \right. \\ \left. + r^2(1 + \kappa_+^2r^2)d\phi^2 + 2\kappa_-\kappa_+r^2(1 - r^2)d\varphi d\phi \right] + dx^i dx^i \quad (3.1)$$

$$F(\varrho) = 1 + \kappa_-^2(1 + \varrho^2) - \kappa_+^2\varrho^2 ; \quad \tilde{F}(r) = 1 + \kappa_-^2(1 - r^2) + \kappa_+^2r^2 \quad (3.2)$$

$$e^{-2\Phi} = e^{-2\Phi_0} \frac{F(\varrho)\tilde{F}(r)}{P(\varrho, r)^2} ; \quad P(\varrho, r) = 1 - \kappa_+^2(\varrho^2 - r^2 - \varrho^2r^2) + \kappa_-^2(1 + \varrho^2)(1 - r^2) \quad (3.3)$$

where we denote the deformation parameters as  $\kappa_{\pm} = \frac{1}{2}(\kappa_L \pm \kappa_R)$ .

The dilaton depends on the choice of the unimodular  $R = \text{diag}(R_L, R_R)$ -matrix, where  $R_L$  and  $R_R$  individually satisfy the modified classical YB equation on the undeformed  $\mathfrak{psu}(1, 1|2)_L$  and  $\mathfrak{psu}(1, 1|2)_R$  of the respective superisometry groups. For the background dilaton (3.3) above, we have the choice of the  $R$ -matrix as  $R_1 = \text{diag}(R_{\mathbb{P}_1}, -R_{\mathbb{P}_1})$ , where  $R_{\mathbb{P}_i}$  are the new  $R$ -matrices obtained using the permutation operators  $\mathbb{P}_i$  on the reference  $R$ -matrix  $R_0$  [42]. Notice that each  $R_{\mathbb{P}_i}$  is associated with the full fermionic Dynkin diagram, and the matrix  $R_1$  is defined on the superisometry algebra  $\mathfrak{psu}(1, 1|2)_L \oplus \mathfrak{psu}(1, 1|2)_R$ .

For our purpose, we choose a particular geodesic, where we set  $x^i = 0$ ,  $r = 0$ ,  $\varphi = \phi = \text{constants}$ . The corresponding metric that the particle feels (in the string frame) is given by

$$ds_3^2 = \frac{1}{F(\varrho)} \left[ -(1 + \varrho^2)(1 + \kappa_-^2(1 + \varrho^2))dt^2 + \frac{d\varrho^2}{(1 + \varrho^2)} + \varrho^2(1 - \kappa_+^2\varrho^2)d\psi^2 \right. \\ \left. + 2\kappa_-\kappa_+\varrho^2(1 + \varrho^2)dtd\psi \right] \quad (3.4)$$

$$F(\varrho) = 1 + \kappa_-^2(1 + \varrho^2) - \kappa_+^2\varrho^2 ; \quad \tilde{F}(r) = 1 + \kappa_-^2 \quad (3.5)$$

$$e^{-2\Phi} = e^{-2\Phi_0} \frac{(1 + \kappa_-^2)}{F(\varrho)}. \quad (3.6)$$

After appropriate rescaling, the metric in the Einstein's frame reads as

$$d\tilde{s}_E^2 = \frac{1}{F^{5/4}(\varrho)} \left[ -(1 + \varrho^2)(1 + \kappa_-^2(1 + \varrho^2))dt^2 + \frac{d\varrho^2}{(1 + \varrho^2)} + \varrho^2(1 - \kappa_+^2\varrho^2)d\psi^2 + 2\kappa_-\kappa_+\varrho^2(1 + \varrho^2)dtd\psi \right]. \quad (3.7)$$

Finally, by introducing a change of variable,

$$1 + \varrho^2 = \cosh^2 \rho \quad (3.8)$$

one can re-express the above metric (3.7) as

$$d\tilde{s}_E^2 = \frac{1}{F^{5/4}(\rho)} \left[ ds_{AdS_3}^2 + ds_{deform}^2 \right] \quad (3.9)$$

$$ds_{AdS_3}^2 = -\cosh^2 \rho dt^2 + d\rho^2 + \sinh^2 \rho d\psi^2 \quad (3.10)$$

$$ds_{deform}^2 = -(-\kappa_- \cosh^2 \rho dt + \kappa_+ \sinh^2 \rho d\psi)^2 \quad (3.11)$$

$$F(\rho) = 1 + \kappa_-^2 \cosh^2 \rho - \kappa_+^2 \sinh^2 \rho. \quad (3.12)$$

Clearly, (3.10) is the usual piece that corresponds to a 2d CFT (on a finite length  $l = 2\pi$ ) associated with the dual Krylov basis [24]. This basis is deformed by the second term (3.11) in the bulk, whose dual interpretation is not very clear at the moment. The boundary of the spacetime is given by the vanishing of the scale factor

$$F(\rho = \rho_B) = 0 \Rightarrow \rho_B = \sinh^{-1} \left( \frac{\sqrt{1 + \kappa_-^2}}{\sqrt{\kappa_+^2 - \kappa_-^2}} \right). \quad (3.13)$$

**Class II background.** The second class background corresponds to a different choice of the unimodular  $R_2 = \text{diag}(R_{\mathbb{P}_1}, -R_{\mathbb{P}_2})$  matrix [42] which corresponds to the background metric as in (3.1). The difference appears in the background dilaton, which is given by

$$e^{-2\Phi} = e^{-2\Phi_0} \frac{F(\varrho)\tilde{F}(r)}{P(\varrho, r)^2}; \quad P(\varrho, r) = 1 - \kappa_+^2 \varrho^2 r^2 + \kappa_-^2 (1 + \varrho^2 r^2). \quad (3.14)$$

Setting  $r = 0$  and following the steps mentioned above in eq.(3.4), we obtain the metric of the subspace in Einstein's frame (after a suitable rescaling) as

$$d\tilde{s}_E^2 = \frac{1}{F^{3/4}(\rho)} \left[ ds_{AdS_3}^2 + ds_{deform}^2 \right] \quad (3.15)$$

where the entities in parentheses are defined in (3.10)-(3.11). Notice that the background (3.15) differs from the previous solution only in the scale factor ( $F(\rho)$ ), which now appears with a different power. However, qualitatively these two solutions should give rise to identical physics when studying the Krylov complexity in the dual CFT.

### 3.2 Operator growth and Krylov complexity

Following [24], we set  $\psi = \text{constant}$ , which yields the massive particle action

$$S = \int dt L ; \quad L = -\frac{m}{F^n(\rho)} \sqrt{K(\rho) \cosh^2 \rho - \dot{\rho}^2} \quad (3.16)$$

$$K(\rho) = 1 + \kappa_-^2 \cosh^2 \rho. \quad (3.17)$$

Notice that the function  $K(\rho)$  sources the deformation of the dual  $SL(2, R)$  Krylov chain on the boundary. In the special case, where the deformation parameters associated with both left and right  $PSU(1, 1|2)$  are identical ( $\kappa_L = \kappa_R$ ), that is,  $\kappa_- = 0$ , we have a situation encountered in the previous section. In other words, this would refer to a background that is conformally equivalent to an  $AdS_2$  subspace that is dual to the  $SL(2, R)$  Krylov chain. Finally, here  $n$  is a free parameter that classifies different supergravity backgrounds, namely  $n = \frac{5}{8}$  for the class I background and  $n = \frac{3}{8}$  for the class II background.

Next, we note down the radial momentum of the particle

$$P_\rho = \frac{m\dot{\rho}}{F^n(\rho) \sqrt{K(\rho) \cosh^2 \rho - \dot{\rho}^2}}. \quad (3.18)$$

The Hamiltonian of the particle, on the other hand, turns out to be

$$H = H_0 = P_\rho \dot{\rho} - L = \frac{m}{F^n(\rho)} \frac{K(\rho) \cosh^2 \rho}{\sqrt{K(\rho) \cosh^2 \rho - \dot{\rho}^2}}. \quad (3.19)$$

Using (3.19), one can simplify the proper momentum (3.18)

$$P_\rho = \frac{H_0 \dot{\rho}}{K(\rho) \cosh^2 \rho}. \quad (3.20)$$

Finally, we note down the equation of motion for  $\rho(t)$  that follows from (3.16)

$$\begin{aligned} & \frac{d}{dt} \left( \frac{1}{F^n(\rho)} \frac{\dot{\rho}}{\sqrt{K(\rho) \cosh^2 \rho - \dot{\rho}^2}} \right) - \frac{n \partial_\rho F}{F^{n+1}(\rho)} \sqrt{K(\rho) \cosh^2 \rho - \dot{\rho}^2} \\ & + \frac{(\partial_\rho K \cosh^2 \rho + K(\rho) \sinh 2\rho)}{2F^n(\rho) \sqrt{K(\rho) \cosh^2 \rho - \dot{\rho}^2}} = 0. \end{aligned} \quad (3.21)$$

Using the constraint (3.19), we can further simplify the above eq.(3.21)

$$\frac{d}{dt} \left( \frac{\dot{\rho}}{K(\rho) \cosh^2 \rho} \right) - \frac{n \partial_\rho F}{\bar{H}_0^2} \frac{K(\rho) \cosh^2 \rho}{F^{2n+1}(\rho)} + \frac{1}{2} \partial_\rho \log K(\rho) + \tanh \rho = 0 \quad (3.22)$$

where  $\bar{H}_0 = \frac{H_0}{m}$  which can be read from eq.(3.19).

Taking into account the fact that near the boundary<sup>3</sup>  $\rho_\Lambda < \rho_B$  and in the limit of small deformation, that is,  $\kappa_-^2 \sim 0$ , together with the fact  $\dot{\rho}(t=0) \ll 1$ , the Hamiltonian

---

<sup>3</sup>Here, the cut-off is set such that  $\kappa_\pm \cosh \rho_\Lambda < 1$  in the limit where  $\rho_\Lambda \gg 1$  and  $\kappa_\pm \ll 1$ .

$\bar{H}_0 \sim \cosh \rho_\Lambda \gg 1$  is a large number. In other words, it is legitimate to drop the second term in (3.22) and solve the rest of the equation, which can be expressed as

$$\frac{d^2}{dt^2} \tanh \rho - \frac{d}{dt} \tanh \rho \frac{d}{dt} \log K + \frac{1}{2} \partial_\rho K + K \tanh \rho = 0. \quad (3.23)$$

Two points should be noted here. First, the solution of (3.23) is the same for both classes I and II backgrounds since their information is hidden in the function  $F(\rho)$  which appears in the NLO in the expansion  $1/\bar{H}_0^2$ . Second, the solution depends on one of the parameters  $\kappa_-$  that appears through the function  $K(\rho)$ . In other words, in the limit  $\kappa_- = 0$ , we have a situation identical to that of [24], which yields a solution of the form<sup>4</sup>

$$\tanh \bar{\rho}(t) = \tanh \rho_\Lambda \cos t. \quad (3.24)$$

In the presence of the deformation and considering it to be small enough<sup>5</sup>  $\kappa_-^2 \ll 1$ , we can find an approximate solution of (3.23). We propose a solution of the form

$$\tanh \rho = \tanh \bar{\rho} + \kappa_-^2 y(t) + \mathcal{O}(\kappa_-^4). \quad (3.25)$$

The equation at  $\mathcal{O}(\kappa_-^2)$  takes the following form

$$\frac{d^2 y}{dt^2} + y = 0 ; \Rightarrow y(t) = A \cos t + B \sin t. \quad (3.26)$$

To fix these constants, we notice that in the presence of YB deformations,  $\rho(t=0) = \rho_\Lambda$ , which yields  $A = 0$ . Therefore, one is left with the remaining constant  $B = \frac{\dot{\rho}(0)}{\kappa_-^2 \cosh^2 \rho_\Lambda}$ , which is fixed in terms of the non-zero velocity at the boundary.

Therefore, the complete solution at NLO reads

$$\tanh \rho = \tanh \rho_\Lambda \cos t + \kappa_-^2 B \sin t. \quad (3.27)$$

Using (3.27), we finally express the proper momentum (3.20) as

$$P_\rho / H_0 = \frac{(\kappa_-^2 B \cos t - \tanh \rho_\Lambda \sin t)}{(1 + \kappa_-^2 D(t))} \quad (3.28)$$

$$D^{-1} = 1 - (\kappa_-^2 B \sin t + \tanh \rho_\Lambda \cos t)^2. \quad (3.29)$$

Considering an expansion in the deformation parameter  $\kappa_-^2 \sim \kappa_L - \kappa_R$ , we obtain

$$P_\rho / H_0 = -\tanh \rho_\Lambda \sin t + \kappa_-^2 \left( B \cos t - \frac{\tanh \rho_\Lambda \sin t}{\tanh^2 \rho_\Lambda \cos^2 t - 1} \right) + \mathcal{O}(\kappa_-^4) \quad (3.30)$$

<sup>4</sup>Notice that, setting  $\kappa_- = 0 = \frac{1}{2}(\kappa_L - \kappa_R)$  does not ensure that the deformations  $\kappa_{L,R}$  are individually zero; this could be one of the possibilities, but the other possibility is that they are equal, namely  $\kappa_L = \kappa_R$  [42]. At LO in  $1/\bar{H}_0^2$  expansions, these two situations cannot be differentiated at the level of the equations of motion. At NLO, these effects can be differentiated in the presence of the parameter  $\kappa_+ = \frac{1}{2}(\kappa_L + \kappa_R)$ . However, a non-zero  $\kappa_-$  certainly corresponds to non-vanishing YB deformation which we explore here.

<sup>5</sup>This would correspond to setting the left and the right deformation parameters close to each other, that is,  $\kappa_L \sim \kappa_R$  while both are non-zero,  $\kappa_L \neq \kappa_R \neq 0$ .

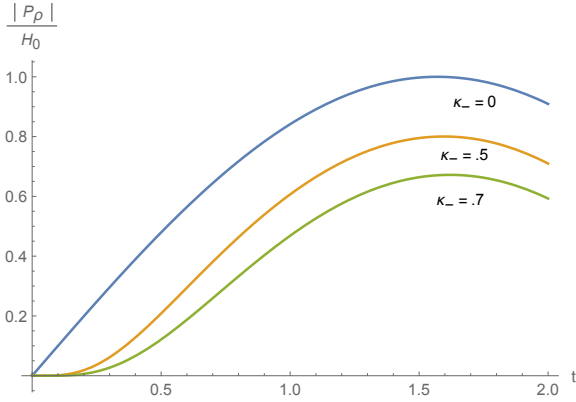


**Figure 3.** We plot proper momentum against time for different choices of the deformation parameter  $\kappa_- = \frac{1}{2}(\kappa_L - \kappa_R)$ , where  $\kappa_L$  and  $\kappa_R$  are close to each other. When they are exactly equal, we have the massive particle experiences an *emerging*  $SL(2, R)$  symmetry which is therefore identical to that of the original notion of the Krylov complexity in a Krylov basis. In our analysis, we set  $B = 0.1$  (which accounts for the initial velocity  $(\dot{\rho}(0))$  of the particle, which is very small to begin with) and  $\rho_\Lambda = 10$ . For  $\kappa_- \neq 0$ , the initial momenta are very small ( $\sim \mathcal{O}(10^{-10})$ ) and cannot be distinguished from the momenta with  $\kappa_- = 0$ , which is actually zero namely  $P_\rho(t = 0)|_{\kappa_- = 0} = 0$ .

where the leading term in (3.30) mimics the result of the undeformed theory [24]. Clearly, setting  $t = 0$ , one finds a non-zero momentum, namely  $P_\rho/H_0 \sim \kappa_-^2 B \ll 1$  in the limit  $\kappa_L \sim \kappa_R$ . This can also be seen from Fig.3, where we plot the proper momentum for different choices of the deformation parameter ( $\kappa_-$ ). Notice that the case  $\kappa_- = 0$  is identical to that of the Krylov complexity [24]. As deformation ( $\kappa_-$ ) increases, the rate of growth is suppressed. In the plot, it is difficult to discriminate between the initial momenta as they are vanishingly small in the range of parameters ( $\rho_\Lambda \gg 1$  and  $B < 1$ ) chosen for the plot.

#### 4 Comments on the mirror model

The mirror dual [52]-[53] of the class II background has been constructed in [42]. Setting  $\kappa_+ = \kappa$  and  $\kappa_- = 0$ , one finds the metric and the background dilaton as

$$ds^2 = -f_1(r)dt^2 + f_2(\varrho)d\varrho^2 + \varrho^2d\psi^2 + f_3(\varrho)d\varphi^2 + f_4(r)dr^2 + r^2d\phi^2 + (dx^i)^2 \quad (4.1)$$

$$f_1(r) = \frac{(1 + \kappa^2 r^2)}{(1 - r^2)} ; \quad f_2(\varrho) = \frac{(1 + \varrho^2)^{-1}}{(1 - \kappa^2 \varrho^2)} ; \quad f_3(\varrho) = \frac{(1 - \kappa^2 \varrho^2)}{(1 + \varrho^2)} ; \quad f_4(r) = \frac{(1 - r^2)^{-1}}{(1 + \kappa^2 r^2)} \quad (4.2)$$

$$e^{-2\Phi} = e^{-2\Phi_0} \frac{(1 - r^2)(1 + \varrho^2)}{(1 - \kappa^2 \varrho^2 r^2)^2}. \quad (4.3)$$

Comparing, for example, the  $tt$  component of the metric in (3.1) and in (4.1), one finds that they can be identified (with  $\kappa_- = 0$ ) under transformation  $\varrho \rightarrow \varrho/\kappa$ ,  $\tilde{\kappa} = 1/\kappa$  and thereby identifying  $\varrho \leftrightarrow r$ . On a similar note, the background dilaton in (3.14) can be mapped to (4.3), which is an artifact of the mirror duality.

For the geodesic under consideration, we set  $\phi = \varphi = x^i = 0$ , which reveals the metric in the string frame as

$$ds_{string}^2 = -f_1(r)dt^2 + f_2(\rho)d\rho^2 + \rho^2d\psi^2 + f_4(r)dr^2. \quad (4.4)$$

For the point particle geodesic, one has to work with the metric in Einstein's frame

$$d\tilde{s}_E^2 = e^{-\frac{\Phi}{2}}ds_{string}^2. \quad (4.5)$$

#### 4.1 Krylov basis and geodesic motion

The Krylov basis can be obtained following a double Wick rotation  $t \rightarrow -i\psi$  and  $\psi \rightarrow it$  and thereby considering an expansion close to  $r \sim 0$ . The above operation corresponds to a rotation of the cylinder by  $\frac{\pi}{2}$ , which converts any timelike interval to a spacelike interval. The Euclidean time has periodicity  $\beta = 2\pi$ , which therefore corresponds to a  $CFT_2$  at a finite temperature [24]. Using the map (3.8), the corresponding metric (4.5) is given by

$$d\tilde{s}_E^2|_{r \sim 0} = h(\rho)(d\psi^2 + f_2(\rho)d\rho^2 - \sinh^2 \rho dt^2) \quad (4.6)$$

$$h(\rho) = \sqrt{\cosh \rho}; \quad f_2(\rho) = (1 - \kappa^2 \sinh^2 \rho)^{-1} \quad (4.7)$$

which clearly reveals a *conformal* Krylov basis for  $\psi = 0$  and  $\kappa = 0$ . On the other hand, for small deformations ( $\kappa \ll 1$ ), one deviates from the Krylov basis.

In order to describe the trajectory of the particle, we parametrize the curve with the choice  $\rho = \rho(t)$  and  $\psi = 0$ . This yields the following action for the massive particle

$$S = \int dt L; \quad L = -m\sqrt{h(\rho)}\sqrt{\sinh^2 \rho - f_2(\rho)\dot{\rho}^2}. \quad (4.8)$$

Like before, we have a cut-off  $\rho_B = \sinh^{-1}(1/\kappa)$  in the bulk and the trajectory of the particle (and hence the action (4.8)) is valid only in the domain  $\rho < \rho_B$ .

The Hamiltonian constraint is given by

$$H = H_0 = P_\rho \dot{\rho} - L = \frac{m\sqrt{h(\rho)}\sinh^2 \rho}{\sqrt{\sinh^2 \rho - f_2(\rho)\dot{\rho}^2}}. \quad (4.9)$$

The equation of motion that follows from (4.8) can be expressed as

$$\begin{aligned} \frac{d}{dt} \left[ \frac{\sqrt{h(\rho)}f_2(\rho)\dot{\rho}}{\sqrt{\sinh^2 \rho - f_2(\rho)\dot{\rho}^2}} \right] + \frac{1}{2\sqrt{h(\rho)(\sinh^2 \rho - f_2(\rho)\dot{\rho}^2)}} & \left[ \partial_\rho h \sinh^2 \rho \right. \\ & \left. + h(\rho) \sinh 2\rho - (\partial_\rho h f_2(\rho) + h(\rho)\partial_\rho f_2)\dot{\rho}^2 \right] = 0 \end{aligned} \quad (4.10)$$

which is equivalent to solving the constraint condition (4.9).

Inverting the constraint eq.(4.9), we obtain

$$\dot{\rho}^2 = \frac{\sinh^2 \rho}{f_2(\rho)} \left[ 1 - \frac{h(\rho)}{\bar{H}_0^2} \sinh^2 \rho \right]; \quad \bar{H}_0 = \frac{H_0}{m}. \quad (4.11)$$

The above eq.(4.11) should be solved with the boundary condition  $\dot{\rho}(t=0) \ll 1$ . From the constraint condition (4.9), this implies  $\bar{H}_0 \sim \sinh \rho_\Lambda \gg 1$  where  $\rho_\Lambda < \rho_B$  is the UV cut-off such that  $\kappa \sinh \rho_\Lambda < 1$ . Therefore, exactly at LO, we have an equation

$$\dot{\rho} = \frac{\sinh \rho}{\sqrt{f_2}} = \sinh \rho \sqrt{1 - \kappa^2 \sinh^2 \rho} + \mathcal{O}(1/\bar{H}_0^2) \quad (4.12)$$

where we consider only the absolute value of the radial velocity.

For the undeformed ( $\kappa = 0$ ) case, one recovers the results of the Krylov basis [24]

$$\tanh \bar{\rho} = \frac{\tanh \rho_\Lambda}{\cosh t}. \quad (4.13)$$

Taking a derivative with respect to time ( $t$ ) and thereby setting  $t = 0$ , one should be able to recover one of the boundary conditions, namely  $\dot{\rho}(t = 0) = 0$ . In the presence of YB effects ( $\kappa \neq 0$ ), one deviates from the solution (4.13) pertaining to a Krylov basis, and instead the solution depends on the deformation parameter ( $\kappa$ )

$$\rho = \bar{\rho}(t) + \kappa^2 y(t) + \mathcal{O}(\kappa^4). \quad (4.14)$$

The equation corresponding to  $y(t)$  turns out to be

$$\dot{y} = \coth t y(t) - \frac{1}{2} \sinh^{-3} t \quad (4.15)$$

where we set  $\tanh \rho_\Lambda \approx 1$ , in the limit  $\rho_\Lambda \gg 1$ .

The corresponding solution has a regular and a divergent piece. The divergent piece has a geometrical origin, which comes from the singularity in the metric (4.6)-(4.7) near the location of the holographic screen. This can be normalized by adding appropriate counter term in the point particle action (4.8). The finite part, on the other hand, reads as

$$y(t) = c_1 \sinh t - \frac{\cosh t}{3}. \quad (4.16)$$

Taking the derivative with respect to time and setting  $t = 0$  afterwards, we find the initial radial velocity along the geodesic of the particle to be non zero  $\dot{y}(0) = c_1$ .

## 4.2 Proper momentum and Krylov complexity

The proper radial distance ( $\bar{\rho}$ ) is defined as the distance between two nearest points along the radial direction ( $\rho$ ) of the geodesic for a fixed time  $\Delta t = 0$  together with  $\Delta\psi = 0$ .

From (4.6), this implies that

$$ds^2 = d\bar{\rho}^2 = h(\rho) f_2(\rho) d\rho^2 \Rightarrow d\bar{\rho} = \frac{\sqrt{h(\rho)}}{\sqrt{1 - \kappa^2 \sinh^2 \rho}} d\rho \quad (4.17)$$

which upon integration yields solution in terms of the Appell function of the first kind,

$$\begin{aligned} \bar{\rho} = & -\frac{\sqrt{2}}{\kappa^2} F_1 \left( \frac{1}{2}; \frac{1}{2}; \frac{3}{8}; \frac{3}{2}; \frac{1}{2} \left( -\kappa^2 \cosh(2\rho) + \kappa^2 + 2 \right), \frac{-\cosh(2\rho)\kappa^2 + \kappa^2 + 2}{2(1 + \kappa^2)} \right) \\ & \times \sqrt[4]{\cosh \rho} \operatorname{csch}(2\rho) \left( \frac{\kappa^2 \cosh^2 \rho}{\kappa^2 + 1} \right)^{3/8} \sqrt{\kappa^2 \sinh^2 \rho (\kappa^2(-\cosh(2\rho)) + \kappa^2 + 2)}. \end{aligned} \quad (4.18)$$

Proper momentum is defined as the canonical momentum defined along the proper radial coordinate ( $\bar{\rho}$ ) of the geodesic

$$P_{\bar{\rho}} = \frac{\partial L}{\partial \dot{\bar{\rho}}} = P_{\rho} \frac{\partial \dot{\rho}}{\partial \dot{\bar{\rho}}} = \frac{m \sqrt{f_2(\rho) \dot{\rho}}}{\sqrt{\sinh^2 \rho - f_2(\rho) \dot{\rho}^2}} = \frac{H_0 \sqrt{f_2(\rho) \dot{\rho}}}{\sqrt{h(\rho)} \sinh^2 \rho} \quad (4.19)$$

where in the last equality, we have used the constraint (4.9).

Expanding (4.19) up to  $\mathcal{O}(\kappa^2)$ , we obtain

$$\begin{aligned} -P_{\bar{\rho}}/H_0 &= \sinh t \sqrt[8]{\tanh^2 t} - \frac{\kappa^2}{16} \sqrt[8]{\tanh^2 t} \text{cschtsecht} \\ &\quad \times (4c_1 \sinh^3 t (6 \cosh(2t) + 7) - 7 \cosh t - \cosh(5t)) + \mathcal{O}(\kappa^4). \end{aligned} \quad (4.20)$$

An expansion close to  $t \sim 0$  reveals a finite contribution as well as a divergent contribution. The divergent contribution has its source in the metric singularity, which can be regularized by adding a counter term, as mentioned before. A closer inspection reveals that this divergence has its origin in the term  $\sqrt{f_2}$  in (4.19). Considering the finite contribution, we find up to LO in the expansion in the YB parameter

$$-P_{\bar{\rho}}/H_0 = t^{5/4} \left( 1 + \left( \frac{5}{8} - \frac{13}{4} \frac{\delta y}{\delta t} \Big|_{t=0} \delta t \right) \kappa^2 \right) + \dots \quad (4.21)$$

which clearly reveals that the complexity is suppressed due to deformations in space time. Notice that this suppression has its origin in the initial velocity of the particle near the boundary, which is a typical characteristic of YB deformation, as we have witnessed before. A closer comparison with [24] reveals that the scaling at an early time (for  $\kappa = 0$ ) differs by a factor  $t^{1/4}$ , which has its origin in the overall scale factor  $h^{1/4}(\bar{\rho})$  appearing in (4.19).

## 5 Summary and conclusions

We identify the dual Krylov basis for a class of Yang-Baxter (YB) deformed supergravity backgrounds that have been constructed in recent years. We consider three different examples of such deformed backgrounds containing and  $\text{AdS}_2$  and  $\text{AdS}_3$  factor for the first two categories and a mirror dual of the (deformed)  $\text{AdS}_3$  solution. In the first example of the deformed  $\text{AdS}_2$  solution, the geometry appears to be conformally equivalent to a Krylov basis. In the second example of deformed  $\text{AdS}_3$ , the Krylov basis is identified at a special point of the parameter space where both left and right deformation parameters appear to be the same, namely  $\kappa_L = \kappa_R$ . The Krylov basis associated with the mirror dual has been identified following a double Wick rotation and setting the deformation parameter to zero.

The key features of our analysis are the following: (i) We show that the effects of YB deformation is to produce a finite cut-off (the so called holographic screen) in the bulk, which from the perspective of an observer living at the boundary is to measure a non-zero growth of Krylov complexity to begin with. In the the bulk this corresponds to a finite initial velocity of the particle, unlike the case with pure AdS. (ii) We show that the rate of growth of complexity is suppressed with increasing YB deformation, which is an artifact of the reduced size of the Hilbert space associated with the Krylov basis.

**Some remarks about the dual QFT.** Here, we outline the nature of the dual field theory for each of the cases studied in this paper. In the example of the deformed  $AdS_2 \times S^2 \times T^6$ , the background (2.8) is conformally equivalent to a  $CFT_1$ . The conformal factor  $\Omega(\rho)$  introduces a finite cut-off (2.9) along the bulk radial direction ( $\rho$ ). One should think of this dual theory as  $(0+1)d$  quantum mechanics (QM) with a cut-off, which eventually breaks the underlying scale invariance at short distances. Here, the holographic screen acts like a physical cut-off regulating the UV divergences in the theory, see Fig.1.

The QM with a cut-off (that lives on the holographic screen) should be thought of as the low energy “effective description” of the  $CFT_1$  living on the boundary ( $\rho_\infty$ ) of the undeformed  $AdS_2$ , which is obtained by integrating out the bulk degrees of freedom between the boundary ( $\rho_\infty$ ) and the cut-off ( $\rho_B$ ) or equivalently integrating out degrees of freedom above this UV cut-off scale,  $\Lambda_{UV} = \frac{1}{\kappa L}$ . The take home lesson from holography is that  $\Lambda_{UV}$  would affect the complexity of this low energy effective theory. Since we break the  $SL(2, R)$  invariance by introducing a cut-off, therefore, the notion of Virasoro generators is no longer applicable. This makes the construction of the Krylov basis quite non trivial for the dual quantum mechanical model under consideration and requires a deeper investigation.

In the example of the deformed  $AdS_3 \times S^3 \times T^4$  solution in the bulk, the dual field theory can be interpreted as a  $CFT_2$ , which is deformed by a *heavy* operator ( $\mathcal{O}(t)$ ) which is dual to a massive particle probe inserted near the boundary.

Using this “heavy probe approximation”, the action can be schematically expressed as

$$S_{tot} = S_{CFT_2} + \kappa_-^2 \int dt \mathcal{O}(t) J(t). \quad (5.1)$$

Notice that the deformation (5.1) acts like a relevant one which puts the theory on the “holographic screen” situated at some interior radial location inside the bulk. Clearly, in this “heavy probe approximation”, the deformation is dictated by the deformation parameter  $\kappa_- \sim (\kappa_L - \kappa_R)$ , which vanishes at the special point where both left and right deformation parameters agree namely,  $\kappa_L = \kappa_R$ . At this special point and modulo  $1/\bar{H}_0^2$  corrections (see discussion below eq. (3.23)), we recover the original Krylov basis pertinent to a  $CFT_2$  [24].

Before we conclude, we wish to list down a set of projects that might be worth pursuing.

- It would be interesting to extend the above analysis for YB deformed solutions containing a deformed  $AdS_n$ , where  $n > 3$ . An ideal example is the Jordanian deformed AdS solution in type IIB [46], which is constructed using  $R$ -matrices that satisfy the classical YB equation. The complete solution can be characterized in terms of the 10d metric containing a deformed  $AdS_5$  factor times a  $S^5$ , along with the background NS-NS and RR fluxes. Interestingly, the background dilaton ( $\Phi$ ) appears to be zero, which therefore does not play a role in the particle dynamics as one goes from the string frame to the Einstein frame.
- The above results could be further generalized for a class of YB deformed string backgrounds generated through  $R$ -matrices that contain two or three parameter generalization [44]. The three parameter deformed backgrounds are in particular of interest as they can be obtained following a Tst and S duality, starting from the undeformed  $AdS_5 \times S^5$ .

**Acknowledgements.** The author would like to thank Carlos Nunez for his comments on the draft. The author acknowledges the Mathematical Research Impact Centric Support

(MATRICS) grant (MTR/2023/000005) received from ANRF, India.

## References

- [1] J. Maldacena, S. H. Shenker and D. Stanford, “A bound on chaos,” *JHEP* **08**, 106 (2016) doi:10.1007/JHEP08(2016)106 [arXiv:1503.01409 [hep-th]].
- [2] D. E. Parker, X. Cao, A. Avdoshkin, T. Scaffidi and E. Altman, “A Universal Operator Growth Hypothesis,” *Phys. Rev. X* **9**, no.4, 041017 (2019) doi:10.1103/PhysRevX.9.041017 [arXiv:1812.08657 [cond-mat.stat-mech]].
- [3] A. Dymarsky and M. Smolkin, “Krylov complexity in conformal field theory,” *Phys. Rev. D* **104**, no.8, L081702 (2021) doi:10.1103/PhysRevD.104.L081702 [arXiv:2104.09514 [hep-th]].
- [4] A. Avdoshkin, A. Dymarsky and M. Smolkin, “Krylov complexity in quantum field theory, and beyond,” *JHEP* **06**, 066 (2024) doi:10.1007/JHEP06(2024)066 [arXiv:2212.14429 [hep-th]].
- [5] T. Anegawa, N. Iizuka and M. Nishida, “Krylov complexity as an order parameter for deconfinement phase transitions at large  $N$ ,” *JHEP* **04**, 119 (2024) doi:10.1007/JHEP04(2024)119 [arXiv:2401.04383 [hep-th]].
- [6] D. Stanford and L. Susskind, “Complexity and Shock Wave Geometries,” *Phys. Rev. D* **90**, no.12, 126007 (2014) doi:10.1103/PhysRevD.90.126007 [arXiv:1406.2678 [hep-th]].
- [7] A. R. Brown, D. A. Roberts, L. Susskind, B. Swingle and Y. Zhao, “Holographic Complexity Equals Bulk Action?,” *Phys. Rev. Lett.* **116**, no.19, 191301 (2016) doi:10.1103/PhysRevLett.116.191301 [arXiv:1509.07876 [hep-th]].
- [8] A. Belin, R. C. Myers, S. M. Ruan, G. Sárosi and A. J. Speranza, “Does Complexity Equal Anything?,” *Phys. Rev. Lett.* **128**, no.8, 081602 (2022) doi:10.1103/PhysRevLett.128.081602 [arXiv:2111.02429 [hep-th]].
- [9] P. Caputa and G. Di Giulio, “Local quenches from a Krylov perspective,” *JHEP* **07**, 164 (2025) doi:10.1007/JHEP07(2025)164 [arXiv:2502.19485 [hep-th]].
- [10] P. Caputa, G. Di Giulio and T. Q. Loc, “Symmetry-Resolved Krylov Complexity,” [arXiv:2509.12992 [hep-th]].
- [11] P. Caputa, H. S. Jeong, S. Liu, J. F. Pedraza and L. C. Qu, “Krylov complexity of density matrix operators,” *JHEP* **05**, 337 (2024) doi:10.1007/JHEP05(2024)337 [arXiv:2402.09522 [hep-th]].
- [12] V. Balasubramanian, P. Caputa and J. Simón, “Variations on a Theme of Krylov,” [arXiv:2511.03775 [hep-th]].
- [13] L. Susskind, “Why do Things Fall?,” [arXiv:1802.01198 [hep-th]].
- [14] L. Susskind, “Complexity and Newton’s Laws,” *Front. in Phys.* **8**, 262 (2020) doi:10.3389/fphy.2020.00262 [arXiv:1904.12819 [hep-th]].
- [15] A. R. Brown, H. Gharibyan, A. Streicher, L. Susskind, L. Thorlacius and Y. Zhao, “Falling Toward Charged Black Holes,” *Phys. Rev. D* **98**, no.12, 126016 (2018) doi:10.1103/PhysRevD.98.126016 [arXiv:1804.04156 [hep-th]].
- [16] L. Susskind and Y. Zhao, “Complexity and Momentum,” *JHEP* **03**, 239 (2021) doi:10.1007/JHEP03(2021)239 [arXiv:2006.03019 [hep-th]].

- [17] J. M. Magán, “Black holes, complexity and quantum chaos,” *JHEP* **09**, 043 (2018) doi:10.1007/JHEP09(2018)043 [arXiv:1805.05839 [hep-th]].
- [18] J. L. F. Barbon, J. Martin-Garcia and M. Sasieta, “A Generalized Momentum/Complexity Correspondence,” *JHEP* **04**, 250 (2021) doi:10.1007/JHEP04(2021)250 [arXiv:2012.02603 [hep-th]].
- [19] J. L. F. Barbon, J. Martin-Garcia and M. Sasieta, “Proof of a Momentum/Complexity Correspondence,” *Phys. Rev. D* **102**, no.10, 101901 (2020) doi:10.1103/PhysRevD.102.101901 [arXiv:2006.06607 [hep-th]].
- [20] J. L. F. Barbón, J. Martín-García and M. Sasieta, “Momentum/Complexity Duality and the Black Hole Interior,” *JHEP* **07**, 169 (2020) doi:10.1007/JHEP07(2020)169 [arXiv:1912.05996 [hep-th]].
- [21] D. S. Ageev and I. Y. Aref’eva, “When things stop falling, chaos is suppressed,” *JHEP* **01**, 100 (2019) doi:10.1007/JHEP01(2019)100 [arXiv:1806.05574 [hep-th]].
- [22] V. Balasubramanian, P. Caputa, J. M. Magan and Q. Wu, “Quantum chaos and the complexity of Krylov of states,” *Phys. Rev. D* **106**, no.4, 046007 (2022) doi:10.1103/PhysRevD.106.046007 [arXiv:2202.06957 [hep-th]].
- [23] P. Caputa, J. M. Magan and D. Patramanis, “Geometry of Krylov complexity,” *Phys. Rev. Res.* **4**, no.1, 013041 (2022) doi:10.1103/PhysRevResearch.4.013041 [arXiv:2109.03824 [hep-th]].
- [24] P. Caputa, B. Chen, R. W. McDonald, J. Simón and B. Strittmatter, “Spread Complexity Rate as Proper Momentum,” [arXiv:2410.23334 [hep-th]].
- [25] A. Fatemiabhari, H. Nastase, C. Nunez and D. Roychowdhury, “Holographic Krylov complexity in confining gauge theories,” [arXiv:2511.22717 [hep-th]].
- [26] A. Fatemiabhari, H. Nastase and D. Roychowdhury, “Holographic Krylov complexity in  $\mathcal{N} = 4$  SYM,” [arXiv:2511.19286 [hep-th]].
- [27] A. Fatemiabhari, H. Nastase, C. Nunez and D. Roychowdhury, “Holographic Krylov Complexity for Conformal Quiver Gauge Theories,” [arXiv:2512.14812 [hep-th]].
- [28] Z. Y. Fan, “Momentum-Krylov complexity correspondence,” [arXiv:2411.04492 [hep-th]].
- [29] Z. Y. Fan, “Generalised Krylov complexity,” [arXiv:2306.16118 [hep-th]].
- [30] P. Z. He, “Revisit the relationship between Krylov complexity rate and radial momentum,” [arXiv:2411.19172 [hep-th]].
- [31] M. P. Heller, J. Papalini and T. Schuhmann, “Krylov Krylov complexity as holographic complexity beyond JT gravity,” [arXiv:2412.17785 [hep-th]].
- [32] M. P. Heller, F. Ori, J. Papalini, T. Schuhmann and M. T. Wang, “De Sitter holographic complexity from Krylov complexity in DSSYK,” [arXiv:2510.13986 [hep-th]].
- [33] Y. Fu, H. S. Jeong, K. Y. Kim and J. F. Pedraza, “Toward Krylov-based holography in double-scaled SYK,” [arXiv:2510.22658 [hep-th]].
- [34] E. Rabinovici, A. Sánchez-Garrido, R. Shir and J. Sonner, “A bulk manifestation of Krylov complexity,” *JHEP* **08**, 213 (2023) doi:10.1007/JHEP08(2023)213 [arXiv:2305.04355 [hep-th]].
- [35] M. Ambrosini, E. Rabinovici, A. Sánchez-Garrido, R. Shir and J. Sonner, “Operator K-complexity in DSSYK: Krylov complexity equals bulk length,” *JHEP* **08**, 059 (2025) doi:10.1007/JHEP08(2025)059 [arXiv:2412.15318 [hep-th]].

[36] S. Baiguera, V. Balasubramanian, P. Caputa, S. Chapman, J. Haferkamp, M. P. Heller and N. Y. Halpern, “Quantum complexity in gravity, quantum field theory, and quantum information science,” [arXiv:2503.10753 [hep-th]].

[37] P. Nandy, A. S. Matsoukas-Roubeas, P. Martínez-Azcona, A. Dymarsky and A. del Campo, “Quantum dynamics in Krylov space: Methods and applications,” *Phys. Rept.* **1125-1128**, 1-82 (2025) doi:10.1016/j.physrep.2025.05.001 [arXiv:2405.09628 [quant-ph]].

[38] E. Rabinovici, A. Sánchez-Garrido, R. Shir and J. Sonner, “Krylov Complexity,” [arXiv:2507.06286 [hep-th]].

[39] B. Hoare and F. K. Seibold, “Supergravity backgrounds of the  $\eta$ -deformed  $\text{AdS}_2 \times S^2 \times T^6$  and  $\text{AdS}_5 \times S^5$  superstrings,” *JHEP* **01**, 125 (2019) doi:10.1007/JHEP01(2019)125 [arXiv:1811.07841 [hep-th]].

[40] D. Roychowdhury, “Field theory aspects of  $\eta$ -deformed superstring background,” *JHEP* **06**, 161 (2025) doi:10.1007/JHEP06(2025)161 [arXiv:2503.06294 [hep-th]].

[41] B. Hoare, “Towards a two-parameter q-deformation of  $\text{AdS}_3 \times S^3 \times M^4$  superstrings,” *Nucl. Phys. B* **891**, 259-295 (2015) doi:10.1016/j.nuclphysb.2014.12.012 [arXiv:1411.1266 [hep-th]].

[42] F. K. Seibold, “Two-parameter integrable deformations of the  $AdS_3 \times S^3 \times T^4$  superstring,” *JHEP* **10**, 049 (2019) doi:10.1007/JHEP10(2019)049 [arXiv:1907.05430 [hep-th]].

[43] M. de Leeuw, A. Pribytok, A. L. Retore and P. Ryan, “Integrable deformations of  $\text{AdS/CFT}$ ,” *JHEP* **05**, 012 (2022) doi:10.1007/JHEP05(2022)012 [arXiv:2109.00017 [hep-th]].

[44] T. Matsumoto and K. Yoshida, “Yang-Baxter deformations and string dualities,” *JHEP* **03**, 137 (2015) doi:10.1007/JHEP03(2015)137 [arXiv:1412.3658 [hep-th]].

[45] R. Borsato and S. Driezen, “All Jordanian deformations of the  $AdS_5 \times S^5$  superstring,” *SciPost Phys.* **14**, no.6, 160 (2023) doi:10.21468/SciPostPhys.14.6.160 [arXiv:2212.11269 [hep-th]].

[46] I. Kawaguchi, T. Matsumoto and K. Yoshida, “A Jordanian deformation of AdS space in type IIB supergravity,” *JHEP* **06**, 146 (2014) doi:10.1007/JHEP06(2014)146 [arXiv:1402.6147 [hep-th]].

[47] O. T. Engelund and R. Roiban, “On the asymptotic states and the quantum S matrix of the  $\eta$ -deformed  $\text{AdS}_5 \times S^5$  superstring,” *JHEP* **03**, 168 (2015) doi:10.1007/JHEP03(2015)168 [arXiv:1412.5256 [hep-th]].

[48] G. Arutyunov, R. Borsato and S. Frolov, “S-matrix for strings on  $\eta$ -deformed  $\text{AdS}_5 \times S^5$ ,” *JHEP* **04**, 002 (2014) doi:10.1007/JHEP04(2014)002 [arXiv:1312.3542 [hep-th]].

[49] G. Arutyunov, R. Borsato and S. Frolov, “Puzzles of  $\eta$ -deformed  $\text{AdS}_5 \times S^5$ ,” *JHEP* **12**, 049 (2015) doi:10.1007/JHEP12(2015)049 [arXiv:1507.04239 [hep-th]].

[50] O. Lunin, R. Roiban and A. A. Tseytlin, “Supergravity backgrounds for deformations of  $\text{AdS}_n \times S^n$  supercoset string models,” *Nucl. Phys. B* **891**, 106-127 (2015) doi:10.1016/j.nuclphysb.2014.12.006 [arXiv:1411.1066 [hep-th]].

[51] B. Hoare, R. Roiban and A. A. Tseytlin, “On deformations of  $AdS_n \times S^n$  supercosets,” *JHEP* **06**, 002 (2014) doi:10.1007/JHEP06(2014)002 [arXiv:1403.5517 [hep-th]].

[52] G. Arutyunov and S. Frolov, “On String S-matrix, Bound States and TBA,” *JHEP* **12**, 024 (2007) doi:10.1088/1126-6708/2007/12/024 [arXiv:0710.1568 [hep-th]].

- [53] G. Arutyunov and S. J. van Tongeren, “ $AdS_5 \times S^5$  mirror model as a string sigma model,” Phys. Rev. Lett. **113**, 261605 (2014) doi:10.1103/PhysRevLett.113.261605 [arXiv:1406.2304 [hep-th]].
- [54] F. Delduc, M. Magro and B. Vicedo, “An integrable deformation of the  $AdS_5 \times S^5$  superstring action,” Phys. Rev. Lett. **112**, no.5, 051601 (2014) doi:10.1103/PhysRevLett.112.051601 [arXiv:1309.5850 [hep-th]].
- [55] F. Delduc, M. Magro and B. Vicedo, “Derivation of the action and symmetries of the  $q$ -deformed  $AdS_5 \times S^5$  superstring,” JHEP **10**, 132 (2014) doi:10.1007/JHEP10(2014)132 [arXiv:1406.6286 [hep-th]].
- [56] C. Klimcik, “Yang-Baxter sigma models and dS/AdS T duality,” JHEP **12**, 051 (2002) doi:10.1088/1126-6708/2002/12/051 [arXiv:hep-th/0210095 [hep-th]].
- [57] C. Klimcik, “On integrability of the Yang-Baxter sigma-model,” J. Math. Phys. **50**, 043508 (2009) doi:10.1063/1.3116242 [arXiv:0802.3518 [hep-th]].
- [58] R. Borsato and L. Wulff, “Target space supergeometry of  $\eta$  and  $\lambda$ -deformed strings,” JHEP **10**, 045 (2016) doi:10.1007/JHEP10(2016)045 [arXiv:1608.03570 [hep-th]].
- [59] F. Delduc, S. Lacroix, M. Magro and B. Vicedo, “On  $q$ -deformed symmetries as Poisson–Lie symmetries and application to Yang–Baxter type models,” J. Phys. A **49**, no.41, 415402 (2016) doi:10.1088/1751-8113/49/41/415402 [arXiv:1606.01712 [hep-th]].
- [60] F. Delduc, M. Magro and B. Vicedo, “On classical  $q$ -deformations of integrable sigma-models,” JHEP **11**, 192 (2013) doi:10.1007/JHEP11(2013)192 [arXiv:1308.3581 [hep-th]].
- [61] T. Kameyama and K. Yoshida, “Minimal surfaces in  $q$ -deformed  $AdS_5 \times S^5$  with Poincare coordinates,” J. Phys. A **48**, no.24, 245401 (2015) doi:10.1088/1751-8113/48/24/245401 [arXiv:1410.5544 [hep-th]].
- [62] T. Kameyama and K. Yoshida, “A new coordinate system for  $q$ -deformed  $AdS_5 \times S^5$  and classical string solutions,” J. Phys. A **48**, no.7, 075401 (2015) doi:10.1088/1751-8113/48/7/075401 [arXiv:1408.2189 [hep-th]].
- [63] C. Klimcik, “Integrability of the bi-Yang-Baxter sigma-model,” Lett. Math. Phys. **104**, 1095–1106 (2014) doi:10.1007/s11005-014-0709-y [arXiv:1402.2105 [math-ph]].